Microsc. Microanal. 19, 73–78, 2013
doi:10.1017/S1431927612013311

Microscopy AND Microanalysis

A Method for Producing Site-Specific TEM Specimens from Low Contrast Materials with Nanometer Precision

Henrik Pettersson, Samira Nik, Jonathan Weidow, and Eva Olsson*

Microscopy and Microanalysis, Department of Applied Physics, Chalmers University of Technology, SE-412 96 Gothenburg, Sweden

Abstract: A method that enables high precision extraction of transmission electron microscope (TEM) specimens in low contrast materials has been developed. The main idea behind this work is to produce high contrast markers on both sides of and close to the area of interest. The markers are filled during the depositing of the protective layer. The marker material can be of either Pt or C depending on which one gives the highest contrast. It is thereby possible to distinguish the location of the area of interest during focused ion beam (FIB) milling and ensure that the TEM sample is extracted precisely at the desired position. This method is generally applicable and enables FIB/scanning electron microscope users to make high quality TEM specimens from small features and low contrast materials without a need for special holders. We explain the details of this method and illustrate its potential by examples from three different types of materials.

Key words: specimen preparation, low-contrast materials, site-specific, scanning electron microscopy, focused ion beam, lift-out, transmission electron microscopy

Introduction

Obtaining high quality data (imaging and spectroscopy) from transmission electron microscopes (TEMs), especially on the new generation of C_s corrected TEMs, demands specimens with superior quality. The extraction of nanoscale devices and individual microstructural features with a nanoscale precision requires special techniques. One of the handiest instruments for making site specific TEM specimens with potential high quality is the combined focused ion beam/scanning electron microscope (FIB/SEM) (Giannuzzi & Stevie, 1999; Lawrence, 2006), where the FIB is used for machining the sample and the SEM is used for checking and imaging the sample without causing any destructive effects. Although this technique has been used in different fields for many years (Heaney et al., 2001; Langford & Petford-Long, 2001; Li et al., 2006; Mitsuishi et al., 2006; Bals et al., 2007; Edwards et al., 2008; Floresca et al., 2009), it has its own limitations and challenges. For example, the exact position of the area of interest (AOI) can easily be lost due to specimen charging and beam drift. Also, it is very challenging to prepare site-specific specimens from nanostructures ($<$100 nm), such as nanoelectronic devices, as well as samples made of very low contrast materials. In fact, in low contrast materials, it is difficult to find a reference mark that can be used as an indication of when to stop milling or for drift compensation. A possible solution to overcome these difficulties is using location marks, and different methods based on using X-shaped marks have been proposed (Dai et al., 2001; van Leer & Giannuzzi, 2008; Unocic et al., 2008). However, in all of these methods, the location marks are positioned outside of the lamella zone and the specimens are thinned down as much as possible before doing the lift-out procedure. Consequently, this kind of marking does not promote the extraction of nm-size electronic devices because there is a high risk of losing the AOI during the pre-lift-out milling. Reference points in the bulk sample are lost as the TEM specimen is lifted out and transferred to the grid for final thinning, which means that they cannot be used as stop points in specimens with low contrast. It should also be noted that these methods were neither applied to low contrast materials nor to very tiny electronic structures (Dai et al., 2001; Stevie et al., 2001; Schwarz & Giannuzzi, 2004; van Leer & Giannuzzi, 2008; Unocic et al., 2008; Felfer et al., 2011). Nanometer scale FIB sample extraction of carbon nanotube interconnects has been reported (Ke et al., 2009). Nevertheless, in this case Pt was specifically used as a protection cap and not as a high-contrast marker.

In the method that we developed, the location marks are within the lamella zone and hence filled with Pt. They have high contrast and can be used as milling end point marks also for the final thinning. Unlike some other methods where the sample was thinned down to the thickness of less than 100 nm while it was attached to the whole body of the sample (Dai et al., 2001), the major thinning of our specimens takes place after lift-out. This reduces the risk of bending or losing the lamella during the lift-out procedure (Kamino et al., 2005). In other words, we have developed a method that increases both the accuracy and success rate for preparing high quality TEM specimens of low contrast nanoscale and local microstructural features. We have evaluated this method using three different types of structures. The first two structures, artificial grain boundary junctions of high-T_c $YBa_2Cu_3O_{7-\delta}$ (YBCO) and low-T_c $Al/AlO_x/Al$ tunnel junctions, are used in nanoelectronic applications such as superconducting interference devices (SQUIDs) (Hilgenkamp & Mannhart, 2002) and qubits for quantum

Received March 15, 2012; accepted July 6, 2012
*Corresponding author. E-mail: eva.olsson@chalmers.se

Figure 1. Schematic of the location marks, placed on both sides of a grain boundary, which is covered by a protective Pt strip.

computers (Amin et al., 2005; Tan et al., 2005). The third structure was a WC-Co-based cemented carbide with Cr additions (Weidow et al., 2009), a material used for metal cutting applications (Exner, 1979), where there was an interest in analyzing a binder phase grain boundary. The investigated structures had the dimensions of 250–750 nm in width and 50–100 nm in height.

Materials and Methods

The site-specific *in situ* lift-out procedure developed here is based on the regular lift-out technique (Jordan et al., 2002). The extraction was carried out using a FEI Strata 235 Dual Beam (FEI Company, Hillsboro, OR, USA) equipped with gas injection systems, for the possibility of depositing Pt and W, and an Omniprobe needle (Omniprobe, Inc., Dallas, TX, USA acquired by Oxford Instruments, Abingdon, Oxfordshire, UK) for *in situ* lift-out work. In the case of WC-Co-based cemented carbides, the location of the microstructural features to be extracted was found using a LEO Ultra 55 SEM (Carl Zeiss Microscopy GmbH, Jena, Germany) equipped with an HKL electron backscatter diffraction (EBSD) system (HKL Technology A/S, Hobro, Denmark acquired by Oxford Instruments). A Philips CM 200 field emission (FEG) TEM (Philips Electron Optics, Eindhoven, The Netherlands) operated at 200 kV, a FEI Tecnai TEM operated at 200 kV and a probe C_s corrected FEI TITAN 80-300 FEG TEM were used for characterization of the TEM specimens. Final Ar ion polishing of the specimens was performed with a Fischione 1010 Ion Mill (E.A. Fischione Instruments, Inc., Export, PA, USA) using an acceleration voltage of 700 V and 10° angle of incidence.

The principle of the developed method for producing site-specific TEM specimens from low contrast materials with nanometer precision is as follows: (1) the AOI is identified with SEM (i.e., device or grain boundary), (2) a protective cap of Pt is deposited over the AOI by electron beam assisted deposition (EBAD), (3) location marks (Fig. 1) are milled out on either side of the AOI, (4) a second protective layer of Pt is deposited by ion beam assisted deposition (IBAD), (5) the AOI is cut lose, lifted out, and attached on a TEM grid, and (6) thinning of the specimen using the location marks as end detection points (if the marks are originally located along a line, they should appear simultaneously during the final thinning step of the lift-out procedure, otherwise the lift-out specimen has been rotated during the final steps and a rotation is then detected).

$YBa_2Cu_3O_{7-\delta}$ Grain Boundaries

The grain boundary in a 300 nm wide conductor line of a YBCO superconducting quantum interference device (SQUID; Fig. 2a) was located by SEM. A Pt-layer measuring $5 \times 1 \times 0.2$ μm was deposited (Fig. 2b) on top, by EBAD. Three location marks, one horizontal $0.5 \times 0.1 \times 0.5$ μm and two vertical bar-shaped, which were $0.1 \times 1.0 \times 0.5$ μm and $0.1 \times 2.0 \times 0.5$ μm in size, respectively, were subsequently milled on each side of the conductor line (Fig. 2c). The thick protective layer of Pt ($10 \times 3 \times 1.5$ μm) was deposited on top using IBAD. The marks were thus filled with Pt, and the regular lift-out procedure could proceed. The trenches were milled on both sides of the Pt cover. Thereafter, the specimen bar was cut lose underneath and on one side (Fig. 2d). The Omniprobe needle was inserted and soldered to the bar using Pt deposition. The remaining side was cut lose and the bar was free to be extracted by the Omniprobe needle. Then, the rest of the sample could be lowered and removed (Fig. 2e). The next step was to insert the TEM grid and attach the bar to the grid using Pt deposition. The Omniprobe needle was subsequently cut free and retracted (Fig. 2f).

Now the final thinning of the bar could begin. A high current ion beam (1,000 pA) was used to mill the front side of the bar until the first marks were visible. The backside was subsequently milled until a bar thickness of 2 μm of the specimen was reached. The current was lowered to 300 pA, and milling was continued on the front side until the next pair of marks were visible (Fig. 2g). The backside was then again milled until a thickness of 1 μm of the specimen was reached. Subsequently, 100 pA was chosen and the bar was milled until the two last marks became visible (Figs. 2h, 2i). The milling of the backside continued until electron transparency was achieved. Further refinement of the specimen quality was achieved using low kV Ar ion milling (0.7 kV) to reduce surface damage. The location marks are clearly visible in the TEM (Fig. 2k). Figure 2k also verifies that the intended area has been located.

$Al/AlO_x/Al$ Tunnel Junctions

The Al tunnel junctions in a superconducting device, fabricated on a 7×7 mm Si/SiO_x substrate, were located by SEM (Fig. 3a). The junctions had a length of 350 nm, a width of 100–400 nm, and a thickness of 75 nm. There are several difficulties in extracting features this small. Al has a low atomic number that is close to Si and SiO_x giving a low contrast between the film and the substrate and also of the tunnel junction. The risk of losing the AOI is therefore high during the thinning procedure. Our solution is to mark the AOI with precise location marks that give high contrast. Consequently, after the deposition of a protective Pt layer by EBAD with dimensions of $5 \times 1 \times 0.2$ μm, one set of horizontal marks with dimensions of $0.5 \times 0.1 \times 1$ μm was milled on each side of the junction (Fig. 3b). Afterward, a thick protective layer of Pt ($15 \times 3 \times 1.5$ μm) was deposited on top by IBAD. The lift-out procedure and the final thinning of the specimen were performed in the same way as for the YBCO samples. With the help of these high contrast location marks, the AOI could be kept during the final thinning (Fig. 3c) and a high quality TEM specimen was obtained (Fig. 3d).

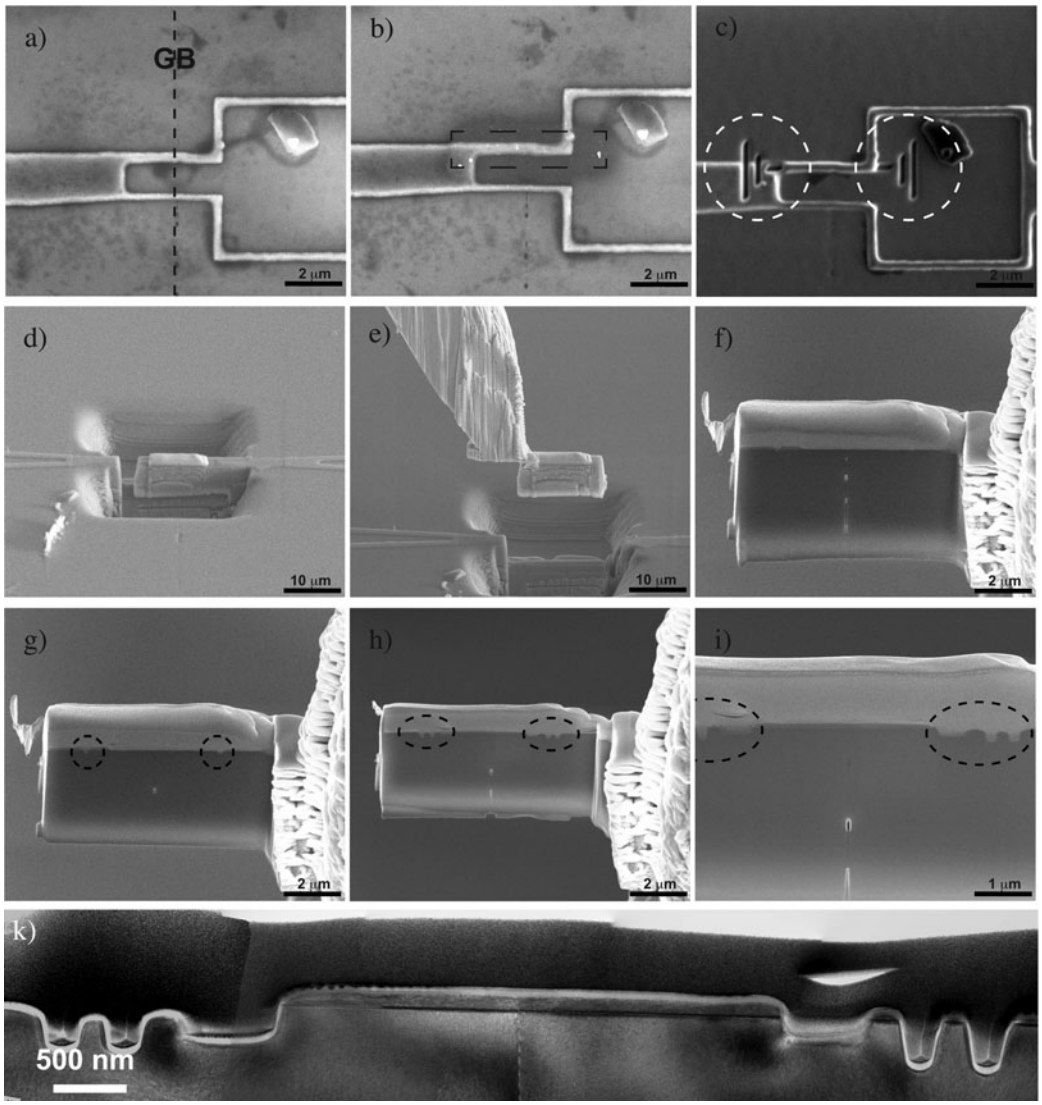

Figure 2. SEM images from the FIB/SEM showing the *in situ* lift-out procedure of the YBCO sample step-by-step, in which (**a**) the AOI is located, (**b**) covered by e-beam assisted Pt deposition (marked with dashed rectangle), (**c**) markers cut out, (**d**) the AOI and the markers are deposited by Pt following the milling of trenches on the sides of the specimen bar, (**e**) the lift-out on the Omniprobe needle, (**f**) lift-out on the TEM grid, and (**g**–**i**) final thinning of the specimen bar. (Milling marks highlighted with dashed ovals.) (**k**) TEM image of the YBCO lift-out specimen with the conductor area, in which the location marks are visible.

Binder Phase Grain Boundaries in WC-Co

An EBSD orientation map from a surface area of 96 μm $\times$ 80 μm was recorded using an initial step size of 80 nm and subsequently refined using a finer step of 30 nm. An area with a binder phase grain boundary approximately 750 nm in length was identified and confirmed (Fig. 4a). The grain boundary area was located in the FIB/SEM (Fig. 4b) and a 6 $\times$ 0.8 $\times$ 0.2 μm protecting EBAD Pt layer was deposited with the long axis oriented perpendicular to the grain boundary (Fig. 4c). On each side of the Pt layer, a square-shaped hole, 0.8 $\times$ 0.8 $\times$ 2 μm, was milled. An additional 15 $\times$ 5 $\times$ 2 μm Pt strip was then deposited by IBAD over the AOI. The thinning procedure was performed from the front side of the specimen bar until both Pt marks became visible (Fig. 4d). It was noted that no contrast of the binder phase grain boundary could be observed. Thinning was then continued from the backside until electron transparency. Further refinement the specimen quality was achieved using low kV Ar ion milling.

Results and Discussion

The successful and reproducible results from three completely different materials (Fig. 5) provide proof of the principle of our method. Figure 5a shows the results of high-resolution TEM of the YBCO specimen, a nm-size feature successfully extracted from a device with dimensions of 5 $\times$ 5 mm. Figure 5b shows a bright-field TEM image of the Al/AlO_x/Al tunnel junctions, and Figures 5c and 5d show dark-field TEM images of the WC-Co speci-

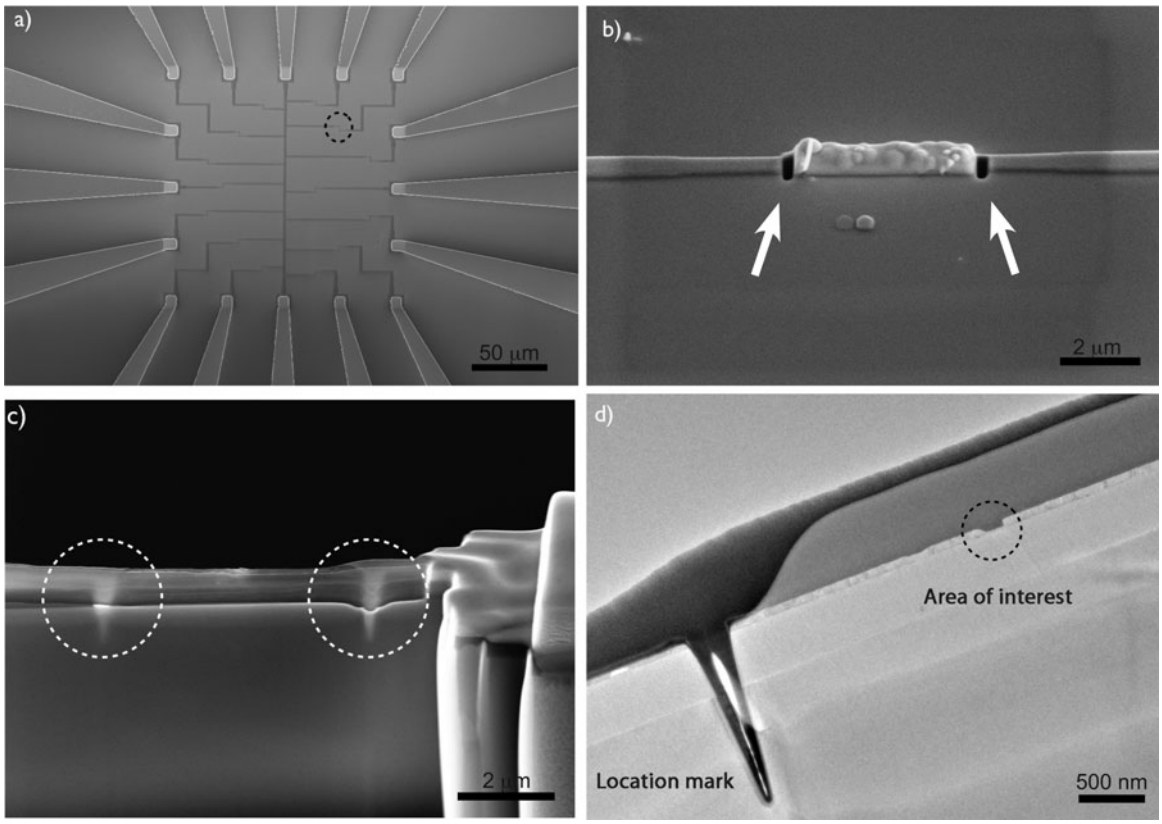

Figure 3. Illustration of the TEM specimen preparation from the Al/AlO_x/Al tunnel junctions. (**a**) SEM image showing the overview of the superconducting device where the location of the Al junction is encircled by a dashed line. (**b**) SEM image of the location marks (arrowed) milled on both sides of the AOI. (**c**) The Pt marks give high contrast in both ion and electron imaging modes in the FIB/SEM (SEM image). (**d**) TEM image of the AOI achieved with the help of location marks.

men where the binder phase grain boundary is present at the top of the specimen. The different character of the samples shows that the method can be applied to any material. It is particularly useful for samples where the feature of interest has a low contrast.

The dimension of the AOIs has been down to 100 nm. However, this is certainly not the limitation of our method. For smaller scale features, particularly for low contrast samples, multiple markers will prevent accidental removal of the AOI in the thinning process of the specimen. A recent method for making atom probe specimens claimed a precision of 50 nm (Felfer et al., 2011). It should be noted that bulk samples were addressed and that the AOI was located using TEM and subsequently trimmed using FIB. In contrast, our samples only have one single individual feature that should be extracted from a macroscopic sample. This requires highly accurate identification of the feature and thinning before being studied in TEM. Another technique for making site-specific specimens is FIB/scanning TEM (STEM) (Kamino et al., 2005). In this method a FIB-TEM compatible specimen holder is used to check the FIB specimen in the TEM and locate the AOI. However, the FIB-TEM compatible specimen holder is a limiting factor because it is not generally available. Our method is independent of additional special holders or attachments. A site-specific specimen can be prepared in any FIB/SEM without the need for a special holder, and there is also no need to check the specimen in a TEM prior to extraction of the AOI.

The limiting factor of the precision in locating small features in our method is the restriction of the dimension and shape of the milled profile of the location marks. Smaller line width and a 90° trench edge of the markers would further improve the precision. The need for high precision markers close to the AOI is caused by the low contrast. Other site-specific techniques do not require special marking or the marks can be located outside of the lamella because the samples have big dimensions or the AOI has high contrast in the FIB (Unocic et al., 2008; Felfer et al., 2011). In our case we have used Pt as the marker material to introduce contrast. However, it should be noted that C could replace Pt in cases where Pt would give low contrast. Other deposition materials are also available and allow an optimal choice of marker material (Reyntjens & Puers, 2001).

Furthermore, this method allows the possibility of returning to a specific location with a higher precision if a milling process has to be interrupted and continued at a later stage. This method is also useful for *ex situ* lift-out where the specimen is thinned down to electron transparency prior to extraction. The possibilities to either choose Pt or C as marker material make the method generic.

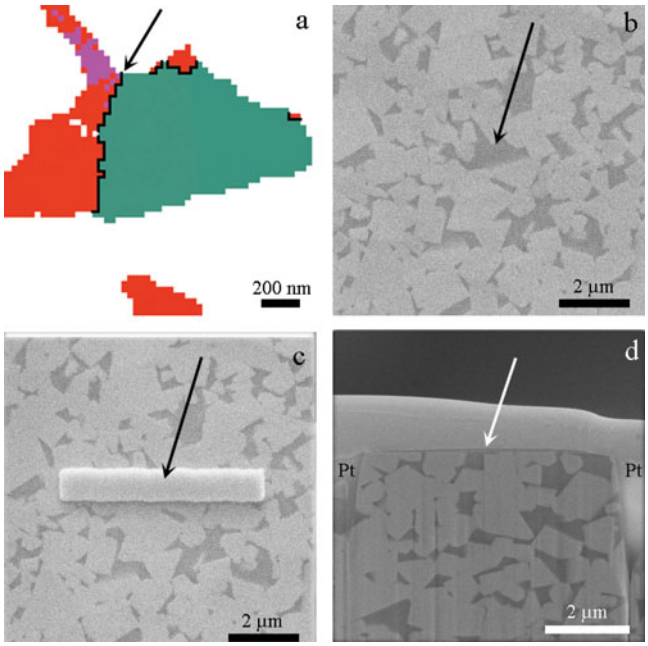

Figure 4. Preparation of a TEM specimen with a binder phase grain boundary for a cemented carbide material. In all images the arrow shows the location of the grain boundary. (**a**) EBSD reconstruction of the binder phase grains (green and orange) with the grain boundary (black). (**b**) SEM image of the corresponding area. WC grains appear bright and the Co based binder phase dark. (**c**) SEM image of Pt deposition across the binder phase grain boundary. (**d**) SEM image of the TEM specimen from the FIB/SEM.

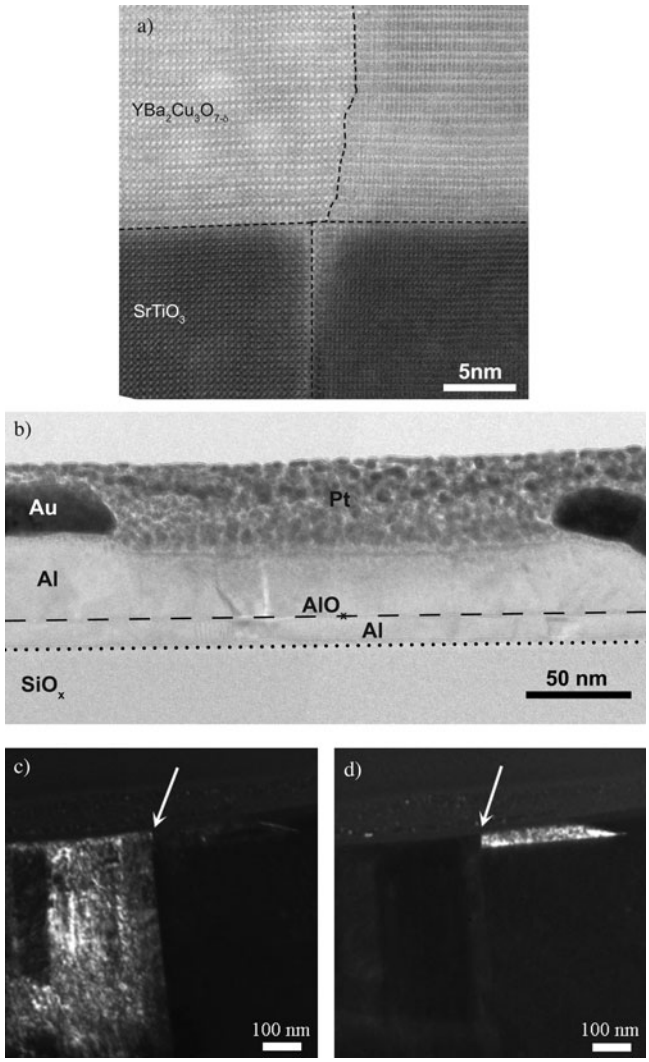

Figure 5. (**a**) High-resolution STEM image of the grain boundary in the superconducting YBCO conductor line; the left YBCO grain is viewed along [110] and the right along [100]. (**b**) TEM bright-field image of the desired $Al/AlO_x/Al$ junction. The AlO_x layer is marked with a dashed line and the Al/SiO_x interface with a dotted line. (**c**) TEM dark-field image of the WC-Co specimen showing one of the binder phase grains (orange in Fig. 4a). (**d**) TEM dark-field image showing the second binder phase grain (green in Fig. 4a).

Conclusions

We have developed a method to extract site-specific TEM specimens with higher precision compared to other known methods. The success rate for site-specific lift-out has increased, and advanced imaging and spectroscopy of these areas have been performed. The precision of this method makes it possible to locate and extract structures in the nanometer range. Also, we have shown that the method is applicable to many different types of structures including both nanodevices and bulk materials. It is particularly useful for low contrast materials where the AOI can otherwise be lost during the preparation procedure.

Acknowledgments

We gratefully acknowledge the Knut and Alice Wallenberg Foundation, the SSF program OXIDE, the Swedish research Council (VR), Sandvik Tooling AB, and Seco Tools AB for financial support.

References

Amin, M.H.S., Smirnov, A.Y., Zagoskin, A.M., Lindström, T., Charlebois, S.A., Claeson, T. & Tzalenchuk, A.Y. (2005). Silent phase qubit based on d-wave josephson junctions. *Phys Rev B* **71**, 064516.

Bals, S., Tirry, W., Geurts, R., Yang, Z. & Schryvers, D. (2007). High-quality sample preparation by low kV FIB thinning for analytical TEM measurements. *Microsc Microanal* **13**, 80–86.

Dai, J.Y., Tee, S.F., Tay, C.L., Song, Z.G., Ansari, S., Er, E. & Redkar, S. (2001). Development of a rapid and automated TEM sample preparation method in semiconductor failure analysis and the study of the relevant TEM artifact. *Microelec J* **32**, 221–226.

Edwards, H.K., Coe, S.C., Fay, M.W., Scotchford, C.A., Grant, D.M. & Brown, P.D. (2008). Site-specific, cross-sectional imaging of biomaterials and the cell/biomaterial interface using focused ion beam/scanning electron microscopy. *J Phys Conf Ser* **126**, 012097.

Exner, H.E. (1979). Physical and chemical nature of cemented carbides. *Int Met Rev* **4**, 149–173.

Felfer, P., Ringer, S.P. & Cairney, J.M. (2011). Shaping the lens of the atom probe: Fabrication of site specific, oriented specimens and application to grain boundary analysis. *Ultramicroscopy* **111**, 435–439.

Floresca, H.C., Jeon, J., Wang, J.G. & Kim, M.J. (2009). The focused ion beam fold-out: Sample preparation method for transmission electron microscopy. *Microsc Microanal* **15**, 558–563.

Giannuzzi, L.A. & Stevie, F.A. (1999). A review of focused ion beam milling techniques for TEM specimen preparation. *Micron* **30**, 197–204.

Heaney, P.J., Vicenzi, E.P., Giannuzzi, L.A. & Livi, K.J.T. (2001). Focused ion beam milling: A method of site-specific sample extraction for microanalysis of earth and planetary materials. *Am Mineral* **86**, 1094–1099.

Hilgenkamp, H. & Mannhart, J. (2002). Grain boundaries in high-T_c superconductors. *Rev Mod Phys* **74**, 485–549.

Jordan, J., Moore, M. & Young, R. (2002). Omniprobe technical note. Hillsboro, OR: FEI Company.

Kamino, T., Yaguchi, T., Hashimoto, T., Ohnishi, T. & Umemura, K. (2005). FIB micro-sampling technique and a site specific TEM specimen preparation method. In *Introduction to Focused Ion Beams, Instrumentation, Theory, Technique and Practice*, Giannuzzi, L.A. & Stevie, F.A. (Eds.), pp. 229–245. New York: Springer Science+Business Media, Inc.

Ke, X., Bals, S., Negreira, A.R., Hantschel, T., Bender, H. & van Tendeloo, G. (2009). TEM Sample preparation by FIB for carbon nanotube interconnects. *Ultramicroscopy* **109**, 1353–1359.

Langford, R.M. & Petford-Long, A.K. (2001). Preparation of transmission electron microscopy cross-section specimens using focused ion beam milling. *J Vac Sci Technol A* **19**, 2186.

Lawrence, P. (2006). The Dualbeam (FIB/SEM) and its applications—Nanoscale sample preparation and modification. Singapore: PTE Ltd Pacific Tech Centre.

Li, J., Malis, T. & Dionne, S. (2006). Recent advances in FIB-TEM specimen preparation techniques. *Mater Charact* **57**, 64–70.

Mitsuishi, K., Shimojo, M., Tanaka, M., Takeguchi, M., Song, M. & Furuya, K. (2006). TEM sample preparation using a new nanofabrication technique combining electron-beam-induced deposition and low-energy ion milling. *Microsc Microanal* **12**, 545–548.

Reyntjens, S. & Puers, R. (2001). A review of focused ion beam applications in microsystem technology. *J Micromech Microeng* **11**, 287–300.

Schwarz, S.M. & Giannuzzi, L.A. (2004). FIB specimen preparation for STEM and EFTEM tomography. *Microsc Microanal* **10**(Suppl 2), 142–143.

Stevie, F.A., Vartuli, C.B., Giannuzzi, L.A., Shofner, T.L., Brown, S.R., Rossie, B., Hillion, F., Mills, R.H., Antonell, M., Irwin, R.B. & Purcell, B.M. (2001). Application of focused ion beam lift-out specimen preparation to TEM, SEM, STEM, AES and SIMS analysis. *Surf Interf Anal* **31**, 345–351.

Tan, E., Mather, P.G., Perrella, A.C., Read, J.C. & Buhrman, R.A. (2005). Oxygen Stoichiometry and instability in aluminum oxide tunnel barrier layers. *Phys Rev B* **71**, 161401.

Unocic, K.A., Mills, M.J. & Daehn, G.S. (2008). Challenges in preparing aluminum alloys for grain boundary characterization. *Microsc Microanal* **14**(Suppl 2), 556–557CD.

van Leer, B. & Giannuzzi, L.A. (2008). Advances in TEM sample preparation using a focused ion beam. *Microsc Microanal* **14**(Suppl 2), 380–381CD.

Weidow, J., Norgren, S. & Andrén, H.-O. (2009). Effect of V, Cr and Mn additions on the microstructure of WC–Co. *Int J Refract Met Hard Mater* **27**, 817–822.